European Review for Medical and Pharmacological Sciences 2023; 27: 3270-3287

# Beta Elemene induces cytotoxic effects in *FLT3* ITD-mutated acute myeloid leukemia by modulating apoptosis

A. ALAFNAN[1], R. DOGAN[2], O. BENDER[2], I. CELIK[3], A. MOLLICA[4], J.A. MALIK[5], K.R.R. RENGASAMY[6], M.K.B. BREAK[7], W.M.A. KHOJALI[7,8], T.N. ALHARBY[9], A. ATALAY[2], S. ANWAR[1]

[1]Department of Pharmacology and Toxicology, College of Pharmacy, University of Hail, Hail, Saudi Arabia
[2]Biotechnology Institute, Ankara University, Ankara, Turkey
[3]Department of Pharmaceutical Chemistry, Faculty of Pharmacy, Erciyes University, Kayseri, Turkey
[4]Department of Pharmacy, "G. d'Annunzio" University of Chieti-Pescara, Chieti, Italy
[5]Department of Biomedical Engineering, Indian Institute of Technology Ropar, Rupnagar, India
[6]Department of Pharmacology, Laboratory of Natural Products and Medicinal Chemistry (LNPMC), Saveetha Dental College, Saveetha Institute of Medical and Technical Sciences (SIMATS), Chennai, India
[7]Department of Pharmaceutical Chemistry, College of Pharmacy, University of Hail, Hail, Saudi Arabia
[8]Department of Pharmaceutical Chemistry, Faculty of Pharmacy, Omdurman Islamic University, Sudan
[9]Department of Clinical Pharmacy, College of Pharmacy, University of Hail, Hail, Saudi Arabia

*Ahmed Alafnan and Rumeysa Dogan contributed equally to this work*

**Abstract. – OBJECTIVE:** β-Elemene, a sesquiterpene with a broad anti-cancer spectrum, is particularly effective against drug-resistant and complex tumors. It can also be efficient against *FLT3*-expressed acute myeloid leukemia. This research aims to determine whether β-Elemene has cytotoxic effects on *FLT3* ITD-mutated AML cells.

**MATERIALS AND METHODS:** Cytotoxicity, cell morphology, mRNA analysis with apoptotic markers, and analysis of 43 distinct protein markers related to cell death, survival, and resistance were all performed to elucidate its mechanism. Additionally, in order to understand how β-Elemene and *FLT3* interact, molecular docking, molecular dynamics simulations, and computational ADME investigations were performed.

**RESULTS:** β-Elemene exhibited cytotoxic activity against FLT3-mutated MV4-11 and *FLT3* wild-type THP-1 cells, with an $IC_{50}$ of around 25 µg/ml. The molecular studies revealed that β-Elemene inhibited cell proliferation by inducing *p53*, and the involvement of *p21*, *p27*, *HTRA*, and *HSPs* were also demonstrated. The interactive inhibition in proliferation was confirmed via molecular docking and dynamics analyses. β-Elemene occupied the *FLT3* enzymatic pocket with good stability at the *FLT3* active site.

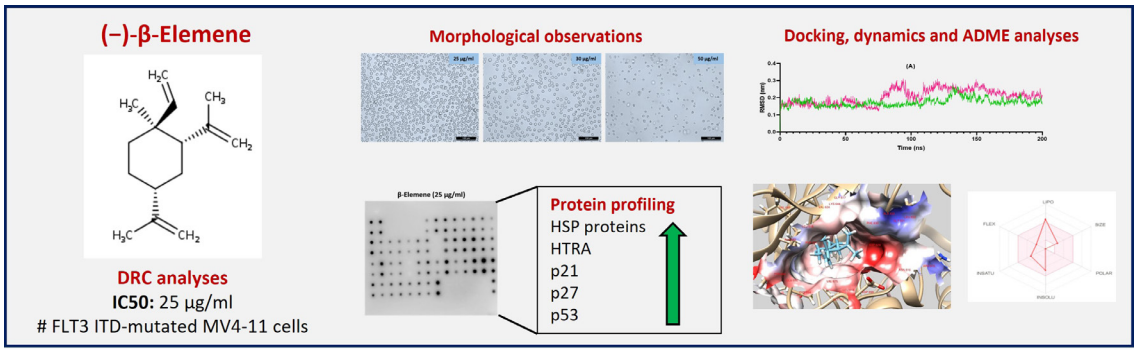


**Graphical Abstract.** Beta Elemene, a sesquiterpene, exhibits cytotoxicity-mediated mechanism against FLT3 ITD-mutated acute myeloid leukemia cells.

*Corresponding Authors:* Sirajudheen Anwar, Ph.D; e-mail: si.anwar@uoh.edu.sa
Onur Bender, Ph.D; e-mail: onur.bender@ankara.edu.tr
Arzu Atalay, Ph.D; e-mail: arzu.atalay@ankara.edu.tr

**CONCLUSIONS: We concluded from our observations that β-Elemene causes cell death in ITD mutant AML cells, together with the effects of stress factors and inhibiting cell division.**

*Key Words:*
Beta elemene, *FLT3*, Acute myeloid leukemia, Molecular dynamics, Cytotoxicity, Natural product, Terpenes.

## Introduction

β-Elemene is a sesquiterpene with a broad anti-cancer spectrum, and it is especially effective against drug-resistant and complex tumors[1]. β is the most predominant one among the three isomers (δ, α, β)[2]. β-Elemene is a component of TCM (Traditional Chinese Medicine) that regulates many molecular targets and produces potential anti-cancer actions[3,4] It was reported that β-Elemene arrests C6 and U87 glioblastoma cells in G0/G1 phase, blocking the proliferation of cells *via MKK3/6-p38* pathway activation and down-regulation of p-*ERK1/2*, *BCL-X/L*, and *BCL-2* pathways[5]. It was also reported that *p38* is activated by the *GMF* overexpression and simultaneously blocks the *ERK1/2* activity in C6 cells[5]. *GMFβ* sensitizes U87 cells to cisplatin by activating *p38*, which signifies *MAPK-GMFβ* signaling cascade in the glioblastoma treatment[6]. In the case of NSCLC H460 and A549 cell lines, β-Elemene was found to increase cisplatin activity by enhancing checkpoint kinase and reducing *CDC2*[7]. Taxanes exhibited moderate synergistic actions along with β-Elemene *in vitro* against prostate and ovarian cancers. The synergistic actions were due to the high expression of *CASP9* and *p53*, enhanced permeabilization of taxanes, micronuclear formation, and binding to efflux pumps[8]. Along with cisplatin treatment, it sensitized cancer cells by decreasing *ERCC* and *XIAP via* Janus Kinase-signaling cascade[9]. Reports claim that β-Elemene enhances the activity of recombinant human endostatin by blocking *MMP-2* and *VEGF*, resulting in a decline in the formation of malignant ascites in the H22 mouse model[10]. Regarding AML, a recent study reported that β-Elemene exhibited cytotoxic activity in *FLT3*-expressing THP-1 cells. It showed a strong cellular inhibition with increasing time and caused beclin-1 mediated and Caspase-dependent mechanism[11]. An emulsion of β-Elemene, harringtonine, aclacinomycin, and Ara-c group formulated by a research group was found to be highly effective and showed a curative effect in the treatment of refractory AML[12]. Another research group synthesized N-(beta-Elemene-13-yl) tryptophan methyl ester, which demonstrated apoptosis in human leukemia HL-60 and NB4 cells with minimal doses of 40 μM[13]. *FLT3* is a member of the class III receptor of tyrosine kinase family. *FLT3* had been detected with the most frequent mutations in AML[14]. Most of the mutations involve ITD in the juxtamembrane domain of *FLT3*, specifically present in AML[15]. The *FLT3* kinase is constitutively activated with the mutations in tyrosine kinase domain and FLT3-ITD. The activation loop and mutations in the *FLT3* juxtamembrane domain can be predicted to result in the loss of auto-inhibitory functionality, activation of *FLT3* kinase, which is constitutive, and its downstream survival signaling cascade like *MAP-Kinase/Ras-ERK/MEK* and *Akt/PI3K* pathways[16]. The mutated *FLT3* also activates the *STAT5* signaling pathway[16]. After the activation of *STAT5*, the target genes for cell growth are induced, like *c-myc* and the anti-apoptotics[17,18]. These investigations indicate that in the aberrant cell growth of leukemia cells, there is a role of *FLT3*-ITD signaling[19,20]. Another research group[21] reported that *Pim-1* expression increased *via* the *FLT3*-ITD pathway, and *FLT3*-ITD is crucial for anti-apoptotic and cell growth events. All the studies concluded that *FLT3*-ITD plays an active role in AML cell growth. β-Elemene can induce anti-cancer effects *via* several pathways, but the mechanism remains unclear[5]. From this point of view, our main starting point was to investigate the interaction of β-Elemene with *FLT3* and to investigate its effectiveness in AML with ITD mutation. We used chemically synthesized (-)-β-Elemene [(1S,2S,4R)-1-Ethenyl-1-methyl-2,4-bis(1-methylethenyl)cyclohexane, (1S,2S,4R)-(-)-2,4-Diisopropenyl-1-methyl-1-vinylcyclohexane), (InChl: 1S/C15H24/c1-7-15(6)9-8-13(11(2)3)10-14(15)12(4)5/h7,13-14H,1-2,4,8-10H2,3,5-6H3/t13-,14+,15-/m1/s] with ≥98.0% purity. To understand the novel molecular pathways in the AML cells, we investigated β-Elemene whether interacts *FLT3* and demonstrate cytotoxic activity against *FLT3* ITD-mutated and *FLT3* wild type AML cells, so that it can be a therapeutic candidate against AML.

## Materials and Methods

### *(–)-β-Elemene*

(−)-β-Elemene[(1S,2S,4R)-1-Ethenyl-1-methyl-2,4-bis(1-methylethenyl) cyclohexane, (1S,2S,

4R)-(−)-2,4-Diisopropenyl-1-methyl-1-vinylcyclohexane] was purchased from Sigma (Cat No.: 63965, Sigma, St. Louis, MO, USA). It's purity ≥98.0% and molecular weight: 204.35. β-Elemene was dissolved in DMSO (Sigma, St. Louis, Missouri, USA) and stored in the dark at 2-8°C.

### Cell Culture

MV4-11 (Cat No.: CRL-9591, *FLT3 ITD*-mutated) and THP-1 (Cat No.: TIB-202, *FLT3* wild type) acute myeloid leukemia cell lines were purchased from ATCC (American Type Culture Collection, Gaithersburg, Maryland, USA). MV4-11 cells were cultured in Iscove's Modified Dulbecco's Medium (Cat No.: 01-058-1A, Biological Industries, Haemek, Israel). THP-1 cells were cultured in RPMI 1640 Medium (ATCC modification) (Cat no: A10491-01, Gibco, Waltham, MA, USA). Both cells' medias were supplemented with 10% heat-inactivated fetal bovine serum (Biowest, Nuaillé, France), 100 U/ml penicillin and 100 µg/ml streptomycin (Gibco, Waltham, MA, USA) and 2.5 µg/ml plasmocin prophylactic (Invivogen, Toulouse, France) in a 37°C cell culture incubator with a humidified atmosphere of 5% $CO_2$. Cells were regularly cultured in polystyrene cell culture flasks with filter cap and subcultured (1:3) when they reached a density above 70%. Cell counting was performed with a hemocytometer and cell viability was also measured by trypan blue (Gibco, Waltham, MA, USA) exclusion method before each main experiment[22].

### Cytotoxicity Assay

Cytotoxic activities of β-Elemene on MV4-11 and THP-1 cell lines were performed with Premix WST-1 Cell Proliferation Assay System (Takara Bio, Shiga, Japan) as we had previously described with slight modifications[23]. 1.0 x $10^4$ cells/well were seeded with 50 µl growth mediums in 96-well cell culture plates. After 24 hours, cells were treated with 1 µg/ml, 5 µg/ml, 10 µg/ml, 15 µg/ml, 20 µg/ml, 25 µg/ml, 50 µg/ml of β-Elemene for 48 or 72 hours. As negative controls, 0.1% DMSO containing growth mediums were used. After incubations with β-Elemene for the indicated times, 10 µl of WST-1 reagent was added to the cells and incubated another 3 hours at cell growth conditions. Absorbances were measured by taking readings at a wavelength of 450 nm with a microplate reader Infinite® 200 PRO (Tecan Life Sciences, Männedorf, Switzerland). For reference reading, 600 nm wavelength was used. $IC_{50}$ values were calculated by using GraphPad Prism 9.2.0. software (GraphPad Software, San Diego, CA, USA).

### Cellular Morphology Analysis

Morphological effects of different doses of β-Elemene on MV4-11 cells were performed by inverted microscope observations as we had previously reported[24]. 5.0 x $10^5$ cells were seeded in 6-well plates in 1 ml growth medium. After 24 hours, cells were treated with 10 µg/ml, 20 µg/ml, 25 µg/ml, 30 µg/ml, and 50 µg/ml of β-Elemene for 48 hours. 0.1% DMSO containing medium was used as untreated control. Cells after treatment with β-Elemene were photographed under an inverted microscope, Leica DM IL LED with DFC-290 camera (Leica, Wetzlar, Germany).

### RNA Extraction and cDNA Reverse Transcription

MV4-11 cells were seeded at a density of 5.0 x $10^5$ cells/well in 6-well plates. 24-hours after plating, cells were treated with 10 µg/ml, 20 µg/ml, 25 µg/ml, and 50 µg/ml of β-Elemene and incubated for 48 hours. After incubation, cells were collected in a 2 ml tube and centrifuged at 1500 rpm for 5 minutes. The cells were then washed with PBS. RNA extraction was performed with miRNeasy Mini Kit (Qiagen, Hilden, Germany) according to the manufacturer's instructions. RNA quantity and quality control were assessed by using NanoDrop 2000 spectrophotometer (Thermo Fisher Scientific, Waltham, MA, USA). One microgram RNA was reverse transcribed by oligo(dT) primers with Transcriptor First Strand cDNA Synthesis Kit (Roche Life Science, Mannheim, Germany). For denaturation of RNA secondary structures, RNA + primer + water mix were incubated at 65°C for 10 minutes. Subsequently added RT reagents and incubated at 30°C for 55 minutes, and at 85°C for 5 minutes in a thermal cycler (Bio-Rad, Hercules, CA, USA) with a heated lid according to the manufacturer's instructions.

### Quantitative Real-time RT-PCR

Quantitative real-time RT-PCR was performed with LightCycler® 480 SYBR Green I Master Mix (Roche Life Science, Mannheim, Germany) at LightCycler® 480 Real-Time PCR device (Roche Life Science, Mannheim, Germany) according to the manufacturer's instructions. Master mix contains FastStart Taq DNA Polymerase, reaction buffer, dNTPs, SYBR Green I dye, and MgCl2. PCR mix was consisted of master mix, forward and reverse primers, PCR grade water with cDNA samples in a total volume of 10 µl. The PCR was performed with initial denaturation at 95°C for 5 minutes, followed by amplification for 45 cycles,

**Table I.** Primer sequences used in quantitative real-time RT-PCR.

| Target | Primers |
|---|---|
| **β-actin** | Forward: 5'-TTCCTGGGCATGGAGTCCT-3' |
| | Reverse: 5'-AGGAGGAGCAATGATCTTGATC-3' |
| **Bax** | Forward: 5'-GGACGAACTGGACAGTAACATGG-3' |
| | Reverse: 5'-GCAAAGTAGAAAAGGGCGACAAC-3' |
| **Bcl-2** | Forward: 5'-ATCGCCCTGTGGATGACTGAG-3' |
| | Reverse: 5'-CAGCCAGGAGAAATCAAACAGAGG-3' |
| **Caspase-3** | Forward: 5'-CAGTGGAGGCCGACTTCTTG-3' |
| | Reverse: 5'-TGGCACAAAGCGACTGGAT-3' |

each cycle consisting of denaturation at 95°C for 10 seconds, annealing at 58°C for 20 seconds, polymerization at 72°C for 20 seconds. The primers were given in Table I. Expression changes were determined by the $2^{-\Delta\Delta CT}$ method. β-Actin was used as house-keeping gene for normalization of expression levels[25].

### Human Apoptosis Antibody Array

Human Apoptosis Antibody Array (Abcam, Cambridge, United Kingdom) was used to investigate the apoptotic mechanism of β-Elemene in ITD-mutated MV4-11 acute myeloid leukemia cells as we previously described[26]. In brief, 5.0 x $10^5$ cells/well were seeded on the 6-well cell culture plate. After 24 hours, cells were treated with 20 μg/ml of β-Elemene or 0.1% DMSO as the control. Cells were incubated with β-Elemene or 0.01% DMSO control for 48 hours, collected, and centrifuged at 1500 rpm for 5 minutes. Supernatant was discarded and cells were washed with PBS. After washing, cells were pelleted and lysed with 400 μl of 1X Lysis Buffer for 30 minutes at 2-8°C on an end-over end-shaker. Then lysate was centrifuged at 14000 rpm for 15 minutes at 4°C and proteins were collected. Total protein quantification was performed with the Pierce BCA Protein Assay Kit (Thermo Fisher Scientific, Waltham, MA, USA) according to the manufacturer's instructions. The membranes of antibody arrays were located on the array container and blocked with 2 ml of 1X Blocking Buffer for 30 minutes at room temperature. After this step, proteins were diluted with 1X Blocking Buffer in an equal concentration and added onto the membranes and incubated overnight at 4°C. Washing were performed with Wash Buffer I and Wash Buffer II and 1 ml of 1X Biotin-conjugated anti-cytokines were added onto membranes and incubated overnight at 4°C. Next day, serial washings were performed and 2 ml of 1X HRP-Streptavidin was pipetted on the membranes and incubated at room temperature for 2 hours. Membranes were washed again and imaged chemiluminescence with Detection Buffer C and D at Odyssey® XF Imaging System (LI-COR Biosciences, Lincoln, NE, USA). The relative intensities were evaluated with Image J software (National Institutes of Health, Bethesda, MD, USA). Normalization of specific protein expressions in each membrane was done according to the following formula:

$$X(Ny) = X(y) * P1/P(y)$$

P1 = mean signal density of Positive Control spots on reference Array
P(y) = mean signal density of Positive Control spots on Array "y"
X(y) = mean signal density for spot "X" on Array for sample "y"
X(Ny) = normalized signal intensity for spot "X" on Array "y"

### In silico Docking Experiments

#### Receptor preparation

The crystal structure of the human *FLT3* co-crystallized with its inhibitor gilteritinib was downloaded from the RCSB database (PDB ID: 6JQR)[27]. The raw file was prepared for the docking experiment by the PrepWizard module of Maestro 11.1 (Schrödinger, New York, NY, USA). The missing chains were added automatically by Prime[27] (Schrödinger, New York, NY, USA), and the protonation state was calculated by PropKa at pH = 7.4. Finally, the receptor-ligand complex was minimized by OPLS-3 force field following a well-established protocol reported by our research group[27-29].

*Docking grid generation*

The docking grid was generated by the Glide module of Maestro[30]. The grid was centered on the crystallographic inhibitor present in the crystal structure and extended to a space of 25 × 25 × 25 Angstrom. The generated grid was used for the docking experiments.

*Self-Docking and validation procedure*

In order to validate the docking procedure, a self-docking experiment was conducted. The crystallographic inhibitor was removed from the receptor, prepared, and minimized by the LigPrep module of Maestro using EpiK at pH = 7.4[31]. The lowest energy structure was used for the self-docking procedure. The obtained ligand was submitted to a first round of docking by using Glide at standard precision accuracy (Glide-SP), then the best raked pose was subjected to a second round of docking by using Glide in eXtra precision (Glide-XP) mode. The RMSD of the best ranked pose was measured as 0.3 Å superimposed to the original crystallographic pose (**Supplementary Figure 1**). Thus, the validated procedure was applied to the docking experiments of β-Elemene.

*Ligands preparation*

β-Elemene was downloaded from zinc database[32] and prepared by the LigPrep module following the same procedure applied to gilteritinib. Then, the best minimized structure was submitted to the docking experiments without further modifications.

*Ligand docking experiments*

The prepared molecule β-Elemene was docked to the *FLT3* enzyme. The first round of docking was performed by Glide in standard precision mode. The best pose generated from the first step was then submitted to the second round of docking by using Glide in eXtra precision accuracy.

*Binding energy estimation*

The best ranked docking pose of β-Elemene was submitted to the binding energy estimation by the MM/GBSA approach in the Prime program of Schrodinger software suite[33] (Schrödinger, New York, NY, USA). MM /GBSA protocol has been applied using default parameters, to calculate the free binding energy of the ligand-enzyme complex in a water environment, employing the variable dielectric surface generalized Born model (VSGB)[34,35] with empirical corrections to hydrogen-bond and π-stacking interactions, to give favorable binding free energy for different protein-ligand complexes[36]. The calculated free binding energies are reported in results section.

### Coulombic Surface Coloring

Coulombic surface coloring calculates electrostatic potential according to Coulomb's law: $\varphi = \Sigma [q_i / (\varepsilon d_i)]$ where φ is the potential (which varies in space), q are the atomic partial charges, d are the distances from the atoms, and ε is the dielectric, representing screening by the medium or solvent. Coulombic surface coloring colors molecular surfaces by the potential values[37]. Red color was set for the lipophilic residues and blue for the polar ones.

### Molecular Dynamics Simulations

Molecular dynamics (MD) simulation was performed with Gromacs version 2020 (GROningen Machine for Chemical Simulations) to analyze the stability of the β-Elemene and *FLT3* complex, and Gilteritinib and *FLT3* complex (PDB ID: 6JQR) to validate and compare the MD simulation. Molecular dynamic system required input files are created by the solution builder tool of CHARMM-GUI web server. The topology file of the β-Elemene, gilteritinib and *FLT3* was generated with the TIP3 water model with an amber FF119SB force field. 10 Å from the surface of the protein center was maintained to define the rectangular system size for simulation. The MD simulations system was neutralized by adding 0.15 M KCl with Monte-Carlo ion placing method. Molecular dynamics simulations are performed in the periodic boundary condition. The system is equilibrated with 0.5 ns NVT and 0.5 ns NPT stages at 1 atm pressure and 303.15 K temperature according to Nose-Hoover[38] thermostat and Parrinello-Rahman barostat[39]. The 200 ns molecular dynamics simulation was now performed with the leap-frog MD integrator. Particle Mesh Ewald (PME) method and linear constraint (LINCS) algorithm were performed to calculate long-range electrostatic interactions and covalent bond constraints, respectively. Trajectory analysis was performed with Gmx scripts, root mean square deviation (RMSD), and root mean square fluctuation (RMSF) measurements were performed. MD trajectory analysis results were created with PyMOL Molecular Graphics System version 2.4.1 and graphics were created with GraphPad Prism 8 (GraphPad Software, San Diego, CA, USA).

### ADME Estimation

The physicochemical properties, lipophilicity such as logP value, water solubility calcula-

tions, pharmacokinetics such as GI absorption and CYP enzyme inhibitor, drug-likeness such as Lipinski, and medicinal chemistry properties such as lead-likeness of the compound β-Elemene were performed with the SwissADME online tool (Swiss Institute of Bioinformatics, Lausanne, Switzerland).

### Statistical Analysis

Differences between groups were evaluated using Student's *t*-test for related part of the study. *p*-values lower than 0.05 were considered statistically significant.

## Results

### Cytotoxicity Profiles of β-Elemene on MV4-11 and THP-1 Cells

Time- and dose-dependent analysis were performed to examine the effects of β-Elemene on acute myeloid leukemia cells with and without *FLT3* mutation. For this purpose, increasing serial doses of β-Elemene were applied to MV4-11 (*FLT3* ITD-mutated) and THP-1 (*FLT3* WT) cells for 48 and 72 hours, and cell viability was measured with the WST-1 cell proliferation assay system at the end of these periods. As seen in Figure 1, considering the effects on both cells, 1, 5, 10 and 15 μg/ml of β-Elemene did not cause an effective inhibition compared to the control, and the inhibition did not go below the green line when the threshold value was accepted as 50% viability. While 20 μg/ml of β-Elemene had no effect on THP-1 cells, it showed an inhibitory effect of 52% in MV4-11 cells at 72 hours. Likewise, 25 μg/ml of β-Elemene was inactive in THP-1 cells for 48 hours and resulted in 17% inhibition at 72 hours. In MV4-11 cells, 25 μg/ml showed 51% and 55% inhibition at 48 and 72 hours, respectively. 50 μg/ml of β-Elemene showed 100% toxicity in both cell lines at all time periods. The cells were completely killed by the effect of this dose. When the activities on the two cells were examined, it was

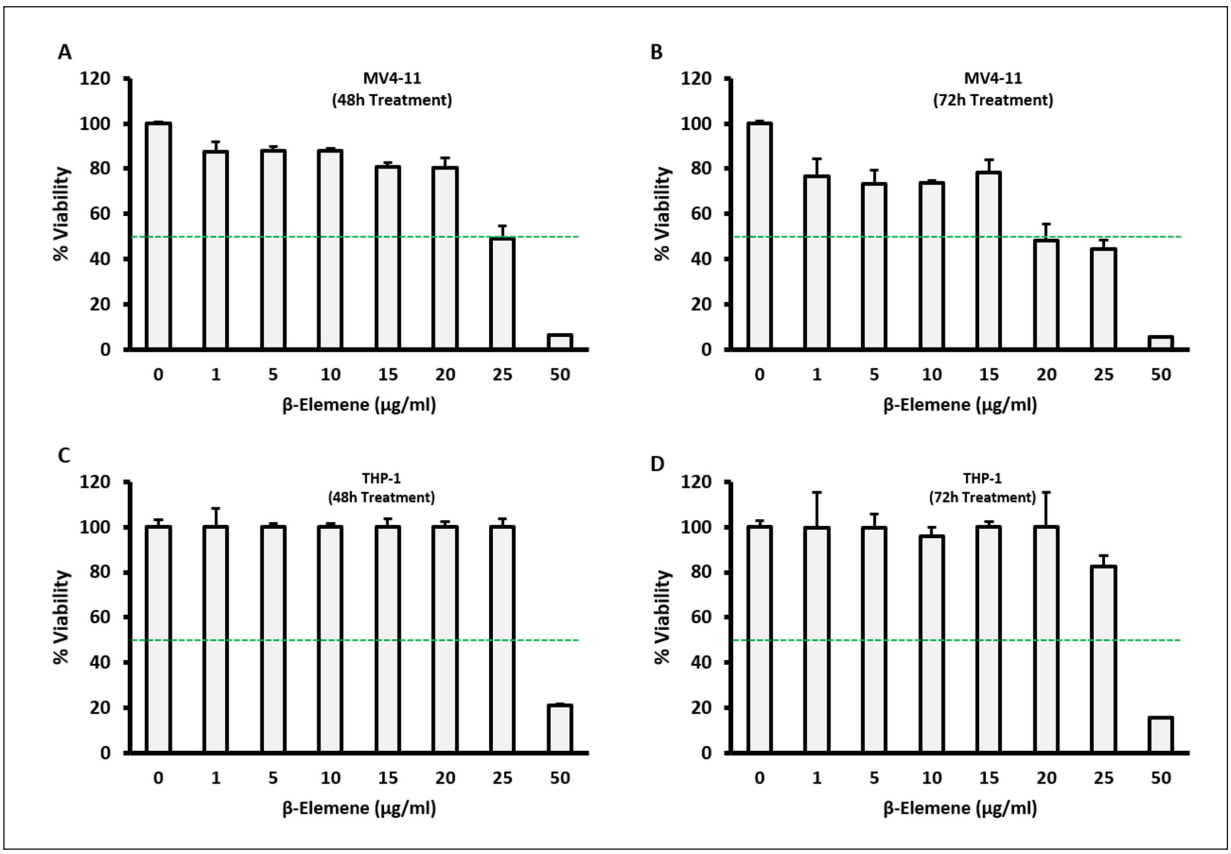


**Figure 1.** Time and dose dependent cellular viability analysis after treatment of β-Elemene. **A**, MV4-11 cells after 48-hours treatment. **B**, MV4-11 cells after 72-hours treatment. **C**, THP-1 cells after 48-hours treatment. **D**, THP-1 cells after 72-hours treatment.

**Table II.** $IC_{50}$ values after 48- or 72-hours treatments of β-Elemene.

| Cell line | 48 hours (µg/ml) | 72 hours (µg/ml) |
|---|---|---|
| **MV4-11** | 25.3 | 20.3 |
| **THP-1** | 27.50 | 29.50 |

observed that β-Elemene was more sensitive to cells carrying the *FLT3*-ITD mutation. In particular, ITD mutant specificity was observed, with the 25 µg/ml dose showing similar inhibitory efficacy at 48 and 72 hours. When all the effect profiles of the doses applied with different serial dilutions were examined, it was determined that β-Elemene has a very narrow therapeutic range on acute myeloid leukemia cells due to its sesquiterpene nature. This can be explained by the dramatic differences between two doses that are particularly close to each other. For further experiments, $IC_{50}$ values were calculated with GraphPad Prism and given in Table II. Further analyses were performed on MV4-11 cells carrying the ITD mutation in the *FLT3* gene.

### Morphological Observations of β-Elemene-Treated MV4-11 Cells

Microscopy analyses were performed to further examine the effects of β-Elemene on MV4-11 cells morphology. Cells were treated with β-Elemene at doses used in cell viability assays for 48 hours and photographed. As seen in Figure 2, consistent with viability assays, 10 and 20 µg/ml of β-Elemene did not alter on cells compared to control. For 25 µg/ml β-Elemene, relatively few cells were observed, while a more stressed phenotype was seen in the cells. An intermediate dose of 30 µg/ml was added to the morphology analysis, and it was determined that the membrane structures of the cells were disrupted, the cell integrity was deterred, and there was a noticeable decrease in the number of cells. 50 µg/ml of β-Elemene, which was determined as 100% toxic dose in cell viability analysis, destroyed the cells completely and the presence of fully dead cells was observed in the area.

### Apoptotic Genes Expression Levels in β-Elemene-Treated MV4-11 Cells

In order to examine the modulations of apoptosis markers during the inhibitory effects of β-Elemene on *FLT3*-ITD cells, changes in mRNA expression levels of major apoptotic genes were analyzed *via* Quantitative real-time RT-PCR. After MV4-11 cells were treated with 10, 20, 25 and 50 µg/ml β-Elemene for 24 hours and 48 hours, total RNA was isolated from cells and RNA quality values were measured. No RNA was obtained in cells treated with 50 µg/ml β-Elemene and it was excluded from this experimental set. RNAs from other doses had desirable quality scores. In this set of experiments, 24-hour treatment was

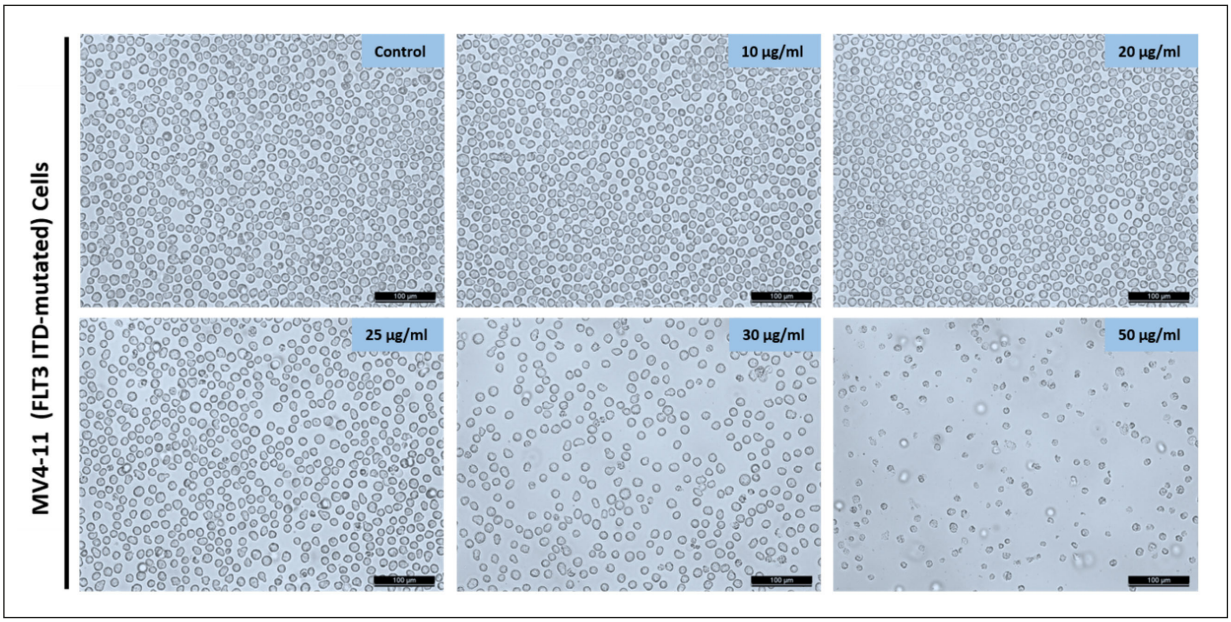


**Figure 2.** Morphological assessment of β-Elemene-treated MV4-11 cells. The cells were treated with different doses of β-Elemene and photographed under an inverted microscope with 200X magnification. Scale bar: 100 µm.

**Table III.** Up-down mRNA regulation status of apoptotic targets after 24 h treatment of β-Elemene.

| | 10 µg/ml | | 20 µg/ml | | 25 µg/ml | |
|---|---|---|---|---|---|---|
| **β-Elemene** | **Fold** | **Status** | **Fold** | **Status** | **Fold** | **Status** |
| **Bax** | -1.34 | Down | -1.41* | Down | -2.00* | Down |
| **Bcl-2** | 1.29* | Up | 1.30 | Up | 1.24 | Up |
| **Caspase-3** | 1.16 | Up | 1.21 | Up | 1.02 | Up |

Comparing to control group. *$p<0.05$.

**Table IV.** Up-down mRNA regulation status of apoptotic targets after 48 h treatment of β-Elemene.

| | 10 µg/ml | | 20 µg/ml | | 25 µg/ml | |
|---|---|---|---|---|---|---|
| **β-Elemene** | **Fold** | **Status** | **Fold** | **Status** | **Fold** | **Status** |
| **Bax** | 2.02* | Up | -1.31* | Down | -1.29* | Down |
| **Bcl-2** | -1.26 | Down | -1.05 | Down | -1.16 | Down |
| **Caspase-3** | 1.09 | Up | -1.03 | Down | 1.08 | Up |

Comparing to control group. *$p<0.05$.

added alongside the standard 48-hour experiment period, to observe potential modulation of cell death at an early stage. *Bax*, *Bcl-2* and *Caspase-3* genes were used as apoptosis markers, and *β*-actin was used as house-keeping gene for normalization. Expression changes were determined by the $2^{-\Delta\Delta CT}$ method. The up-down regulation values were given in Table III and Table IV.

From this, it can be thought that β-Elemene initiates apoptotic resistance mechanism in cells at an early stage. In the *Bcl-2* gene, the fold regulation was in the upward direction for all doses. This was considered as another factor contributing to the resistance mechanism. In the *Caspase-3* gene, upregulation was observed with slight values, although it was not significant ($p>0.05$). For 48-hour treatments, as seen in Table IV, all the *Bcl-2* changes were down-regulated. No significant results were obtained for *Caspase-3* ($p>0.05$). From here, it was observed that β-Elemene developed an apoptotic resistance in MV4-11 cells after the treatment, the resistance continued through the *Bax* gene in the following process, but *Bcl-2* levels decreased over time. These results are consistent with the results published previously on THP-1 cells, as will be discussed in detail in the discussion section. Thus, it can be said that β-Elemene induces cytotoxicity-mediated cell death in AML cells. The mechanism of effective cell death *via* cytotoxicity despite developing resistance is investigated in more detail in the following sections.

### *Apoptosis Array Profile of β-Elemene-treated MV4-11 Cells*

Quantitative real time RT-PCR data suggested that β-Elemene induces cytotoxicity-mediated cell death. For a more comprehensive elucidation of the cell death mechanism, the protein levels of 43 different apoptosis-related targets were analyzed. For this purpose, the Human Apoptosis Antibody Array - Membrane kit was used. With this kit, high-throughput screening of targets that are responsible in cell death, survival and resistance can be performed simultaneously. In this system, where antibodies belonging to different targets are processed on a membrane, also there are positive control spots (Pos) used for normalization, negative control spots (Neg) where antibody dilution buffer is processed and blank spots (BLANK) that do not contain anything. In this study, MV4-11 cells were treated with 25 µg/ml β-Elemene for 48 hours and protein isolation was performed. Growth medium containing 0.1% DMSO was used as control. Two separate membranes were treated with lysates and kit procedures followed. As seen in Figure 3, chemiluminescence images were acquired and quantification of each protein spot was performed. First, with this study, endogenous expression of 43 different genes related to cell survival and death mechanisms were determined in AML cells with *FLT3*+ carrying ITD mutation. In Figure 3A and Figure 3B (array map), it is observed at the band

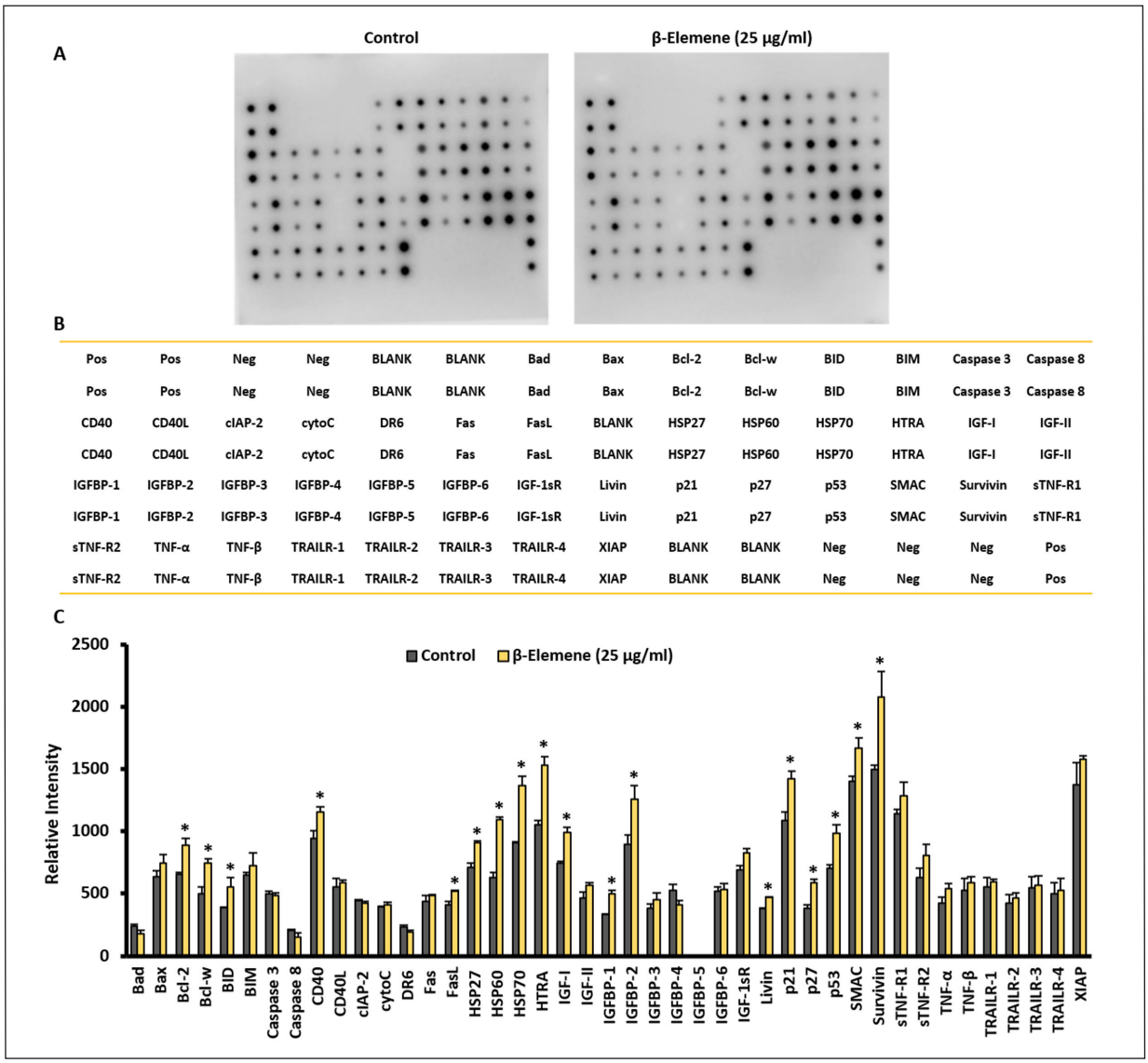


**Figure 3.** Apoptosis-related protein profiling of β-Elemene-treated MV4-11 cells by using human apoptosis antibody array**.** **A**, Chemiluminescence images of array membranes. Left panel: Profile of proteins from untreated control cells. Right panel: Profile of proteins from cells treated with 25 µg/ml β-Elemene for 48 hours. **B**, Array membrane reference map. **C**, Quantification of proteins from the control and treatment groups. *$p<0.05$.

level, and in Figure 3C which protein is found, quantitatively, at what level. As a result of the analysis, it was determined that 18 of 43 protein targets changed in a statistically significant manner. Three of the six members of the *Bcl-2* family (*Bad, Bax, Bcl-2, Bcl-w, BID* and *BIM*) increased significantly. The stress induced by β-Elemene in the cell increased the expression of anti-apoptotic *Bcl-2* and *Bcl-w*, while significantly increased the expression of *BID* from *BH-3* only initiators. In fact, we found here a competitive balance between anti-apoptotic and pro-apoptotic members.

We can say that there are pro-apoptotic responses that try to increase due to other cell signaling mechanisms against the anti-apoptotic response due to cellular stress. Focusing on the cell death mechanism, it was observed that β-Elemene significantly increased the tumor suppressor *p53* expression. More specifically, *p21* and *p27* expressions, which play a role in cell cycle inhibition, were also increased accordingly. From this, it was found that the *p53, p27, p21* axis inhibited cell growth, and *p53* -the *Bax* cofactor- contributed to the pro-apoptotic balance. On the other

hand, protein expressions of *Livin*, *Survivin* and *IGF-I* increased significantly and contributed to the inhibition of apoptosis. Heat shock proteins *HSP27*, *HSP60* and *HSP70* as stress sensitive proteins showed significant increases with treatment of β-Elemene. We also observed an increase in the level of *HTRA* protein, which is involved in apoptosis or drug-associated cytotoxicity. As a result of *cytoC* levels, which did not change, we saw that β-Elemene did not affect the mitochondrial outer membrane, so the expressions of Caspases were not affected. β-Elemene did not affect tumor necrosis factor α and β by as well as *TNF*-related apoptosis-inducing ligand (*TRAIL*) series 1-4. Likewise, other death receptors *Fas* and *DR6* were not significantly altered. *CD40* was increased and this may be related to *TRAFs*. In summary, in AML cells carrying *FLT3*-ITD mutation, 48-hour treatment of 25 μg/ml β-Elemene caused stress on the cells *via HSP* proteins, developed apoptosis resistance through apoptotic inhibitors activation of different pathways and caused cell death with the induction of *p53* also with the contributions of *p21* and *p27* by cell cycle arrest. It did not cause activation of membrane receptors and mitochondrial membrane degradation. In the light of all these data, we can conclude that β-Elemene causes cytotoxicity-mediated cell death in ITD mutant AML cells, together with the stress factors effects and inhibiting cell division.

### Molecular Docking Analyses of β-Elemene and FLT3

In order to better understand the molecular bases of β-Elemene activity as inhibitor of *FLT3*, *in silico* docking experiments were carried out. Our experiments demonstrated that this compound is able to dock in the enzymatic cavity of the enzyme (docking score -6.11); however, β-Elemene has a sesquiterpene type structure, with no heteroatoms able to act as acceptor/donor for hydrogen bonds, thus, the only interactions possible between β-Elemene and the enzyme are hydrophobic. Indeed, in the enzymatic cavity is present a large hydrophobic cluster formed by the following amino acids: Phe 830, Val 624, 675, Leu

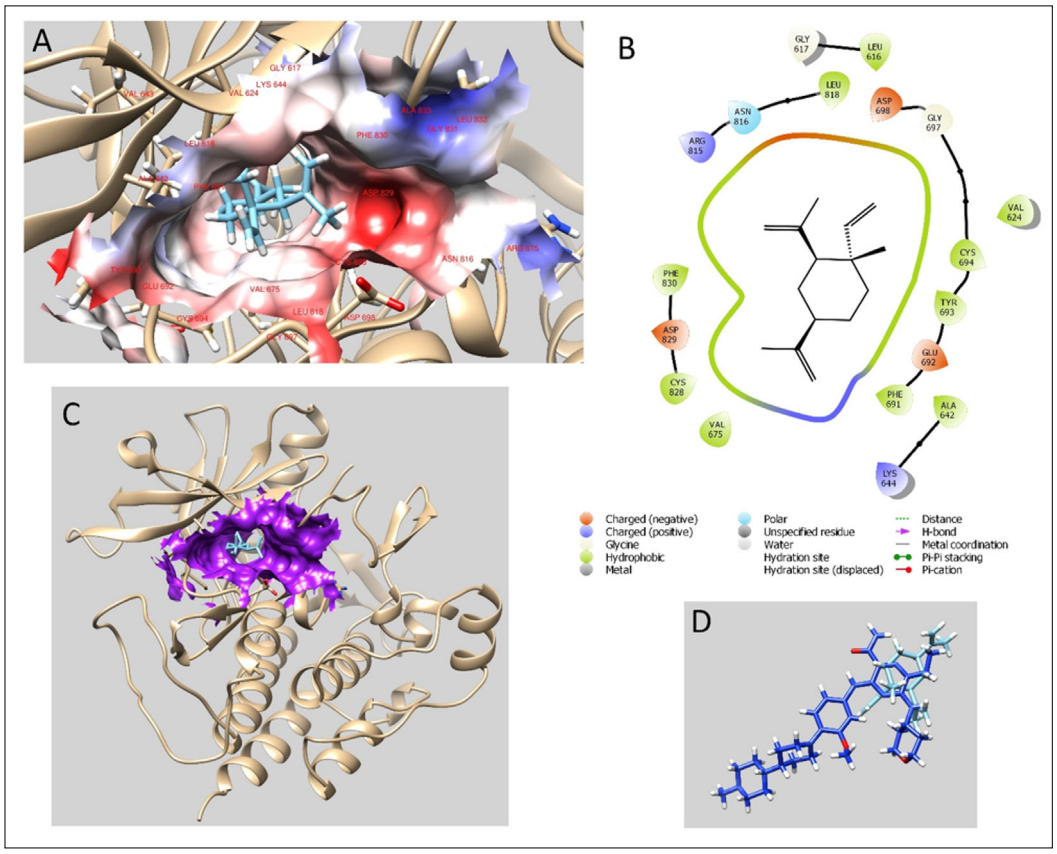


**Figure 4.** Molecular docking analyses of β-Elemene and FLT3. **A**, Coulombic surface colored. **B**, Interaction diagram of β-Elemene docked to *FLT3*. **C**, Best pose of β-Elemene docked to *FLT3*. **D**, β-Elemene superimposed to the crystallographic inhibitor.

616,818,832, Ala 642, 833, Gly 617, Cys 828, 694. The hydrophobic cluster was highlighted by the coulombic Surface coloring method as seen in Figure 4A, embedded in the software UCSF-Chimera (Figures 4B-C). The ΔG-binding energy was also calculated. The value (-27.2 Kcal/mol) is lower than that of the crystallographic ligand (-75.0 Kcal/mol) as expected by the low-energy lipophilic interactions found. However, β-Elemene is able to occupy efficiently the enzymatic pocket occupied by the piranyl-aminopyrazine-carboxamide portion of the crystallographic ligand (docking score -8.10) as depicted in Figure 4D.

### *Molecular Dynamics Simulations of β-Elemene and FLT3 Complex*

Molecular dynamics simulations are used in drug research to reveal the stability and persistence of the protein-ligand complex obtained from molecular docking studies[40,41]. With MD simulations, it is possible to computationally analyze macromolecules at the atomic level in the physiological environment. In this study, the stability of the β-Elemene and *FLT3* complex obtained by docking was investigated by MD simulations. To validate the MD simulation and for comparison purposes, the gilteritinib and *FLT3* complex was run with 200 ns MD under the same conditions as the same β-Elemene and *FLT3* complex. In MD simulations, protein RMSD value below 0.3 nm and being constant indicates that the protein is stabilized. As shown in Figure 5A, both β-Elemene and *FLT3,* and gilteritinib and *FLT3* complex measured RMSD values around 0.2 nm up to 80 nm and below 0.3 nm thereafter. RMSF measurements show fluctuations in protein structure and mobility. A potently bound ligand is expected to reduce the fluctuation of active site residues,

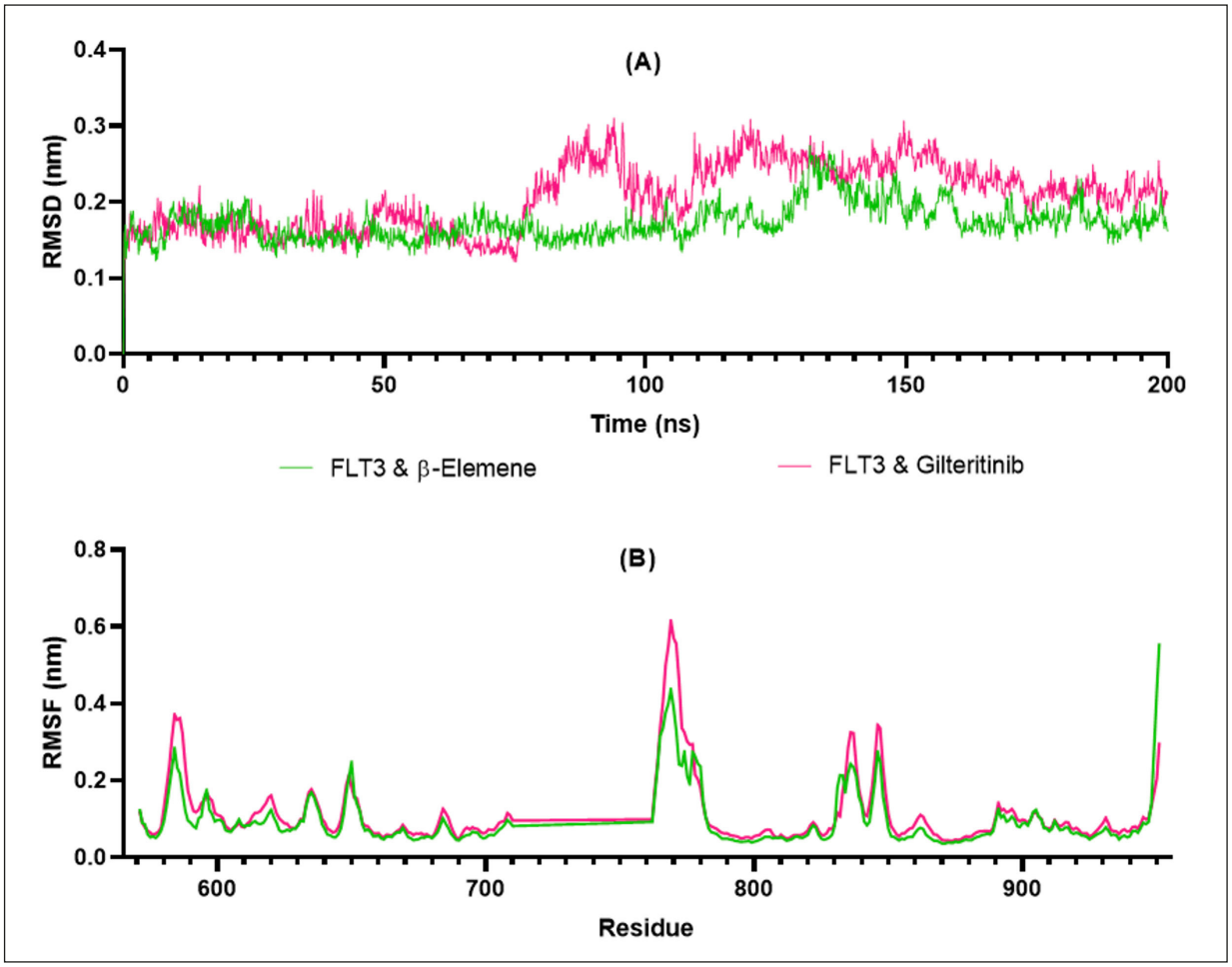


**Figure 5.** Molecular dynamics simulations trajectory analysis of β-Elemene and *FLT3* and gilteritinib and *FLT3* complexes. **A**, Root mean square deviation (RMSD) of compound β-Elemene and cocrystal ligand gilteritinib of *FLT3* (PDB ID: 6JQR). **B**, Root mean square fluctuation (RMSF) of protein-ligand complexes for 200 ns.

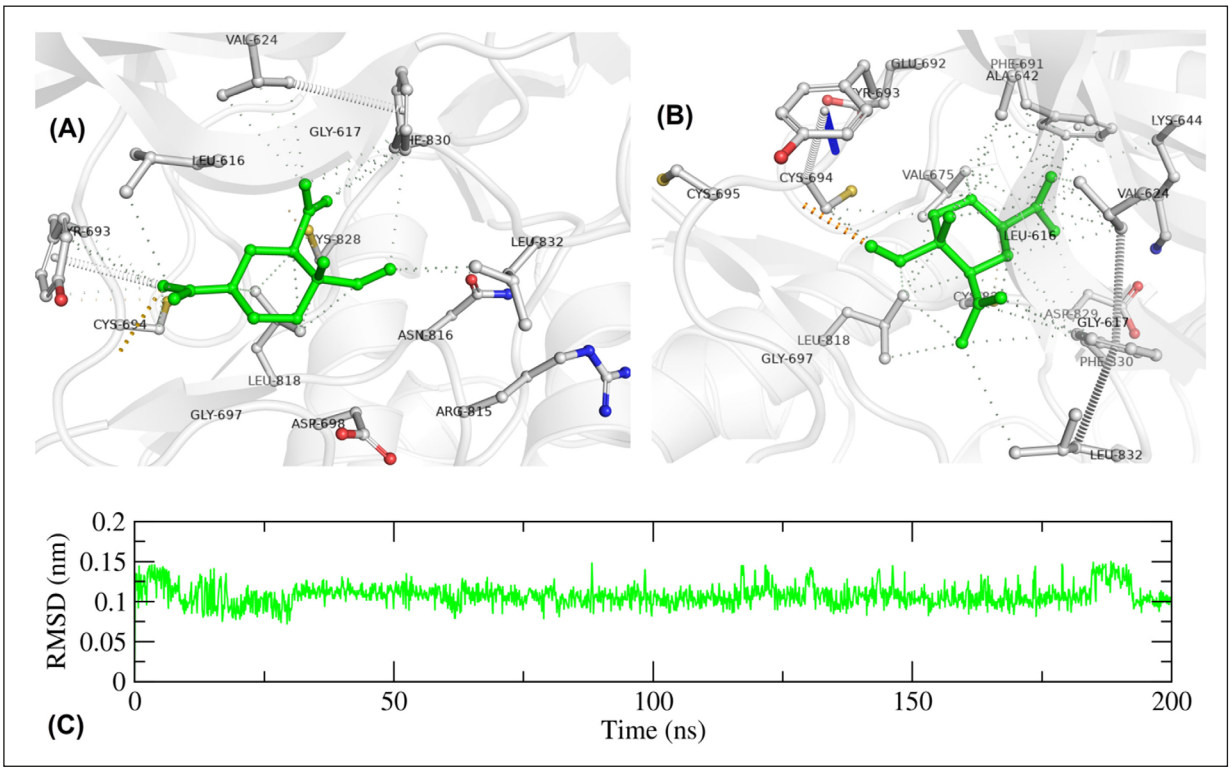


**Figure 6.** Protein-ligand molecular dynamical interactions. **A**, Binding pose of β-Elemene at the active site of *FLT3* in the 100th ns. **B**, binding poses of end of the 200 ns MD simulations. **C**, RMSD graph of β-Elemene at the active site of *FLT3*.

making the structure more compact. As shown in Figure 5B, β-Elemene at amino acids 760-780 and amino acids 830-850 containing active site redundant stabilized the structure from the standard drug gilteritinib. The binding poses at 100 ns in Figure 6A, and the binding pose at 200 ns in Figure 6B are given to show the time-dependent variation of protein-ligand interactions. In addition, the behavior of β-Elemene and *FLT3,* and gilteritinib and *FLT3* complexes for 200 nanoseconds (ns = $10^{-9}$ second) is shown in **Appendix**. As given in Figure 6C, β-Elemene remained stable around 0.1 nm at the *FLT3* active site throughout the MD simulation. Its interaction with residues such as Cys694, Tyr693, Val624, Leu832, Phe830, Gly697, and Leu818 remained stable.

### *Computational ADME Study*

The studies that examine the absorption, distribution, metabolism, and excretion (ADME) events of drugs in the body quantitatively and especially in time dimensions are called pharmacokinetic or ADME calculations. It has been found useful to measure some ADME properties of active molecules computationally in medicinal chemistry. Because many drug molecule candidates do not show a good ADME profile in clinical phase studies, they cannot become drug molecules. Therefore, some physicochemical, lipophilicity, water-solubility, pharmacokinetics, drug-likeness, and medicinal chemistry parameters of the active compound β-Elemene were measured[42]. As shown in Figure 7, the β-Elemene has a structure containing C and H atoms. Since it does not contain atoms such as N, O, and S that add polarity to the structure, its polarity is low, and the TPSA value was measured as 0. Containing β-Elemene C and H, the lipophilic character is high due to its structure, and the consensus LogP value was measured as 4.65[43]. Its solubility in water is between moderate and soluble. It has low GI absorption and can be inhibitor for *CYP2C19* and *CYP2C9*[44]. Because of its potential to inhibit these CYP enzymes, it may interact with drugs heavily used in the treatment of AML and produce adverse effects. Since it deviates from one of the Lipinski rules[45], it is within the acceptable limiting rules. It conforms to the limiting rules of Ghose, Weber, and Egan but not to Muegge[46]. According to the medicinal chemistry characteristics, the structural alert Brenk was measured as 3.63 from 0 to 10

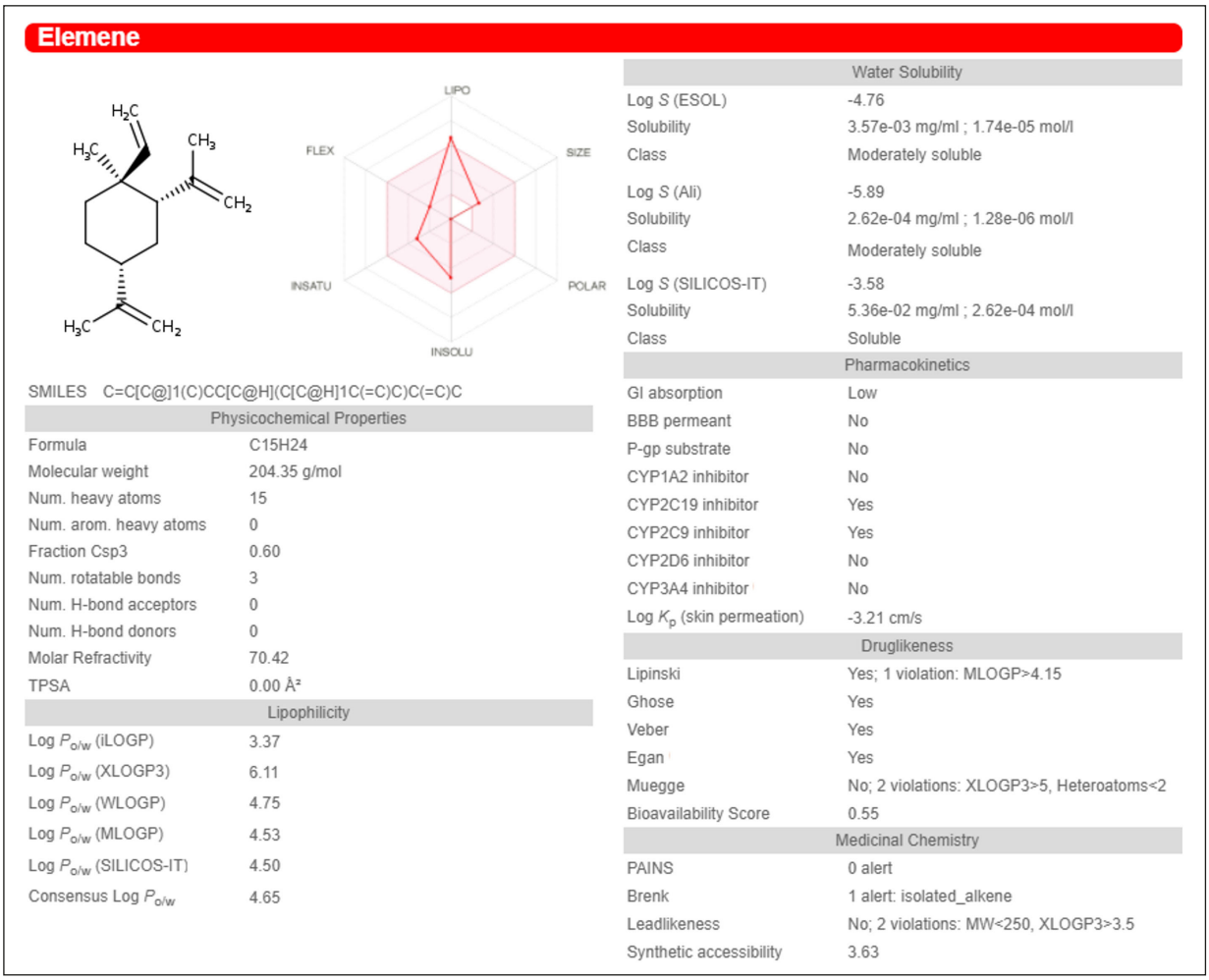


**Figure 7.** ADME properties of β-Elemene calculated *via* SwissADME server.

due to the presence of separated alkanes, compatibility for pan assay interference structure, and ease of synthesis.

## Discussion

The malignancy of AML mainly affects the bone marrow however, malignant cells can also be discovered in the blood. It spreads rapidly and is extremely aggressive[47]. A growing concern regarding the treatment of AML necessitates the investigation of new contemporary therapeutic approaches. β-Elemene is a natural product with promising anti-cancer potential, as evidenced by various research studies. The action of β-Elemene can be mediated by a variety of molecular mechanisms[48]. However, the mechanism is still unclear, particularly in the case of AML with its mutations. In this study, we tested the cytotoxic capability of β-Elemene against both ITD mutant *FLT3* AML cells (MV4-11) and non-mutated AML cells (THP-1 cells). We observed that 25 μg/ml of β-Elemene was partially inactive in THP-1 cells, with 17% inhibition, but 55% inhibition in MV4-11 cells, respectively. We also discovered that β-Elemene suppressed cell growth as concentration increased, with 50 μg/ml totally inhibiting cell growth in MV4-11 and THP-1 cells. According to the literature, Jiang et al[11] found that β-Elemene showed cytotoxic activity in THP-1 cells, which is consistent with our study. In this context, our study has unique value by performing the comparative screening of β-Elemene against *FLT3* WT THP-1 and most importantly *FLT3*-ITD mutant MV4-11 cells. Cytotoxic potential of β-Elemene against glioma cancer cells has also previously been investigat-

ed[49]. They observed that β-Elemene could considerably inhibit glioma cell growth in a dose and time-dependent manner. Several other research studies[2,50-52] have shown that β-Elemene possesses *in vitro* cytotoxicity against numerous cancer cell lines. In this study, we investigated whether there is a change in the expression of *Bax, Bcl-2,* and *Caspase-3* as apoptotic markers for giving a preliminary idea of cell death mechanism. We found that β-Elemene downregulates the Bax gene with the increase in the dose, revealing that the inhibition in proliferation is due to cytotoxicity in the AML cells. After that, we also investigated the expression profile of another major apoptotic marker, *Bcl-2*. We found that with the increase in dose, there were non-significant decrease in the expression of *Bcl-2*. However, to clarify whether a resistance to apoptosis, we investigated any impact on the expression profile of *Caspase-3*. We found slight upregulation in the expression but insignificant. It was also reported that β-Elemene, along with hyperthermia, significantly affects lung cancer cell lines A549. They found that the inhibition occurs due to a decrease in the S phase and inducing apoptosis through an increase in *Bax* and *p21*. They also claimed a decrease in *Caspase-9* and *Bcl-2* expression, which might explain cell death[53]. For a more comprehensive elucidation of the cell death mechanism, the protein-level levels of 43 different cell death-related targets were investigated *via* Human Apoptosis Antibody Array. We observed that out of 43 protein targets, the expression of 18 protein targets changed in a statistically significant way. The stress-induced by β-Elemene in the cell increased the expression of anti-apoptotic *Bcl-2* and *Bcl-w* while significantly increasing *BID* expression from *BH-3* only initiators. Interestingly we observed there a competitive balance between anti-apoptotic and pro-apoptotic members. We also found that β-Elemene significantly increased the tumor suppressor *p53* expression. More specifically, *p21* and *p27* expressions, which play a role in cell growth inhibition, increased accordingly. The *p53, p27*, and *p21* axis inhibited cell proliferation, while *p53* -the *Bax* cofactor- contributed to the pro-apoptotic balance. The anticancer effects of drugs depend on their ability to trigger programmed cell death in cancer cells. Since *p53* plays a great role in controlling cell fate in response to stress DNA damage, the therapeutic strategies ultimately lead to activating *p53* mediated pro-apoptotic pathway causing cell death[54]. We also observed the protein expressions of *Livin, Survivin*, and *IGF-I* increased significantly and contributed to the inhibition of apoptosis as a compensatory mechanism to maintain the homeostasis. Heat shock proteins *HSP27, HSP60,* and *HSP70* as stress-sensitive proteins showed significant increase with the treatment of β-Elemene. It is reported that stress can induce apoptosis *via* numerous independent and dependent mechanisms[11]. The best strategy for causing anti-tumor drug effects is apoptosis or autophagy in tumor cells[55]. It is a degenerative process with both the roles of promotion and suppression of cancer which mostly occur during stress[56-58]. We also observed an increase in the level of *HTRA* protein, which is involved in apoptosis or drug-associated cytotoxicity[59]. So, we here concluded from the data that β-Elemene causes cytotoxicity-mediated cell death in ITD mutant AML cells, together with the stress factors effects and inhibiting cell division. Our results conclude that β-Elemene could be an inhibitor against ITD mutated AML cells. We have demonstrated that β-Elemene has high anti-cancer potential against MV4-11 cell line, which has not been reported before. As reported, β-Elemene has demonstrated the best results against other cancers, both *in vitro* and *in vivo;* so, we propose that β-Elemene should be utilized in combination with other anticancer drugs against AML *in vivo.*

To understand better whether the β-Elemene activity is an inhibitor of *FLT3*, we performed *in silico* docking experiments. Our experiments found that β-Elemene can dock in the enzymatic cavity of the enzyme (docking score -6.11). Although β-Elemene is a sesquiterpene type molecule with no heteroatoms but can act as acceptor/donor for hydrogen bonds; thus, the only association possible between β-Elemene and the enzyme are hydrophobic. However, β-Elemene was found to occupy efficiently the enzymatic pocket occupied by the piranyl-aminopyrazine-carboxamide portion of the crystallographic ligand. This may be the reason that β-Elemene is inhibiting the AML cell proliferation. We also carried out molecular dynamics (MD) simulations to determine whether β-Elemene and the enzyme form a stable complex for the first time. The stability of the β-Elemene and *FLT3* complex was validated *via* MD simulation and for comparison purposes, the gilteritinib and *FLT3* complex was used as a positive control against β-Elemene and *FLT3* complex. In MD simulations, we found that the protein RMSD value

below 0.3 nm and being constant indicates that the protein is stabilized. β-Elemene remained stable around 0.1 nm at the *FLT3* active site throughout the MD simulation. Its interaction with residues such as Cys694, Tyr693, Val624, Leu832, Phe830, Gly697, and Leu818 remained stable. We also carried out ADME studies to find the pharmacokinetics of β-Elemene. It is possible to come across experimental ADME studies of β-Elemene in the literature[60]. In this study, an *in silico* ADME study was conducted to support experimental studies. When we examine the computational ADME literature, we found that in the study by Sankar et al[61], β-Elemene's *in silico* study was performed with the pkCSM server. In our study, calculations were made with the SwissADME server. We have seen that other pharmacokinetic features are the same as pkCSM server except for the inhibitory feature of *CYP2C19* and *CYP2C9* enzymes. Considering the possible adverse effects, it may interact with drugs used extensively in the treatment of AML due to its potential to inhibit CYP enzymes.

This is the first study to determine the efficacy of β-Elemene in *FLT3*-ITD mutated AML cells. This study suggests that β-Elemene has an anti-cancer mechanism on *FLT3*-expressed AML disease through *p53* induction, contributions of *p21* and *p27*, and increased *HTRA* expression. At the same time, significant increase in various stress factors contributes to cytotoxicity-mediated inhibition. However, the limitations of our study are that this study did not examine whether changes in *FLT3*-dependent signaling pathways. Since β-Elemene occupied the *FLT3* enzymatic pocket at the *FLT3* active site with good stability, it will be interesting to see how β-Elemene affects cell signaling pathways involved in *FLT3* expression. So, this study not only illuminated the basis of the relationship between β-Elemene and *FLT3*-expressed AML, but also identified the targets of β-Elemene. Studies with primary AML cells may produce higher resolution data.

## Conclusions

We here demonstrated that β-Elemene, a sesquiterpene, has a considerable cytotoxic potential against *FLT3* expressed and ITD-mutated AML. This is the first investigation into β Elemene's potential for treating *FLT3*-mutated AML, and it could be a promising compound with the ability to modulate critical cell growth inhibitors and stress markers. According to our *in silico* studies, β-Elemene exhibits a good specificity against *FLT3*. It was also deciphered that the β-Elemene has good stability in the *FLT3* mutated enzymatic pocket, this demonstrates that the downstream survival targets are being inhibited, resulting in a decrease in cell proliferation. This is an *in vitro* and *in silico* study to unravel anti-cancer mechanism of β-Elemene against AML, additional studies are required to elucidate further *FLT3*-dependent signaling pathways. Finally, to be validated for human usage, β-Elemene should be tested clinically against AML.

### Acknowledgments
All molecular dynamics simulations reported were performed utilizing TÜBİTAK (The Scientific and Technological Research Council of Turkey), ULAKBİM (Turkish Academic Network and Information Centre), High Performance and Grid Computing Centre (TRUBA) resources. The authors highly thankful to Dr. Ramazan Ceylan from Selcuk University, Turkey for the valuable support. Authors extend their appreciation to Scientific Research Deanship at University of Ha'il - Saudi Arabia through project fund number RG-21 173.

### Funding
This research has been funded by Scientific Research Deanship at University of Ha'il - Saudi Arabia through project number RG-21 173.

### Authors' Contributions
Conceptualization: Ahmed Alafnan, Onur Bender and Sirajudheen Anwar; Data curation: Ahmed Alafnan, Rumeysa Dogan, Onur Bender, Ismail Celik, Adriano Mollica, Jonaid Ahmad Malik, Tareq Nafea Alharby and Sirajudheen Anwar; Methodology: Rumeysa Dogan, Onur Bender, Ismail Celik, Adriano Mollica, Sirajudheen Anwar, Kannan R.R. Rengasamy; Software: Ismail Celik and Adriano Mollica; Supervision: Onur Bender, Arzu Atalay and Sirajudheen Anwar; Writing–original draft: Sirajudheen Anwar, Rumeysa Dogan, Onur Bender, Ismail Celik, Adriano Mollica, Jonaid Ahmad Malik, Kannan R.R. Rengasamy; Writing–review and editing: Onur Bender, Mohammed Khaled Bin Break, Weaam Mohamed Ali Khojali, Arzu Atalay and Sirajudheen Anwar.

### ORCID ID
Onur Bender: 0000-0003-0691-3508
Arzu Atalay: 0000-0003-1309-5291
Sirajudheen Anwar: 0000-0002-0926-2790

### Conflicts of Interest
The authors declare that they have no conflict of interest to declare.

### Availability of Data and Materials
All data generated or analyzed during this study are included in this published article.

### Informed Consent
Not applicable.

### Ethics Approval
Not applicable.

## References


1) Liu J, Zhang Y, Qu J, Xu L, Hou K, Zhang J, Qu X, Liu Y. β-Elemene-induced autophagy protects human gastric cancer cells from undergoing apoptosis. BMC Cancer 2011; 11: 183.
2) Wu XS, Xie T, Lin J, Fan HZ, Huang-Fu HJ, Ni LF, Yan HF. An investigation of the ability of elemene to pass through the blood-brain barrier and its effect on brain carcinomas. J Pharm Pharmacol 2009; 61: 1653-1656.
3) Jiang S, Ling C, Li W, Jiang H, Zhi Q, Jiang M. Molecular Mechanisms of Anti-cancer Activities of β-elemene: Targeting Hallmarks of Cancer. Anticancer Agents Med Chem 2016; 16: 1426-1434.
4) Zhai B, Zhang N, Han X, Li Q, Zhang M, Chen X, Li G, Zhang R, Chen P, Wang W. Molecular targets of β-elemene, a herbal extract used in traditional Chinese medicine, and its potential role in cancer therapy: a review. Biomed Pharmacother 2019; 114: 108812.
5) Zhu T, Xu YY, Dong B, Zhang J, Wei Z, Xu Y, Yao Y. β-elemene inhibits proliferation of human glioblastoma cells through the activation of glia maturation factor β and induces sensitization to cisplatin. Oncol Rep 2011; 26: 405-413.
6) Baldwin RM, Garratt-Lalonde M, Parolin DAE, Krzyzanowski PM, Andrade MA, Lorimer IAJ. Protection of glioblastoma cells from cisplatin cytotoxicity via protein kinase Ciota-mediated attenuation of p38 MAP kinase signaling. Oncogene 2006; 25: 2909-2919.
7) Li QQ, Wang G, Huang F, Li JM, Cuff CF, Reed E. Sensitization of lung cancer cells to cisplatin by β-elemene is mediated through blockade of cell cycle progression: antitumor efficacies of β-elemene and its synthetic analogs. Med Oncol 2013; 30: 488.
8) Zou B, Li QQ, Zhao J, Li JM, Cuff CF, Reed E. β-Elemene and taxanes synergistically induce cytotoxicity and inhibit proliferation in ovarian cancer and other tumor cells. Anticancer Res 2013; 33: 929-940.
9) Li QQ, Lee RX, Liang H, Wang G, Li JM, Zhong Y, Reed E. β-Elemene enhances susceptibility to cisplatin in resistant ovarian carcinoma cells via downregulation of ERCC-1 and XIAP and inactivation of JNK. Int J Oncol 2013; 43: 721-728.
10) Jiang ZY, Qin SK, Yin XJ, Chen YL, Zhu L. Synergistic effects of Endostar combined with β-elemene on malignant ascites in a mouse model. Exp Ther Med 2012; 4: 277-284.
11) Jiang Z, Liu J, Chen B, Mani R, Pugazhendhi A, Shanmuganathan R, Jacob JA. Cytotoxic effects of a sesquiterpene β-elemene on THP-1 leukemia cells is mediated via crosstalk between beclin-1 mediated autophagy and Caspase-dependent apoptosis. Process Biochem 2019; 87: 174-178.
12) Zheng C, Cai X, Wu S, Liu Z, Shi Y, Zhou W. Enhancing effect of β-elemene emulsion on chemotherapy with harringtonine, aclacinomycin, and Ara-c in treatment of refractory/relapsed acute myeloid leukemia. Pak J Med Sci 2014; 30: 1270-1270.
13) Yu Z, Wang R, Xu L, Dong J, Jing Y. N-(beta-Elemene-13-yl)tryptophan methyl ester induces apoptosis in human leukemia cells and synergizes with arsenic trioxide through a hydrogen peroxide dependent pathway. Cancer Lett 2008; 269: 165-173.
14) Takahashi S. Downstream molecular pathways of FLT3 in the pathogenesis of acute myeloid leukemia: biology and therapeutic implications. J Hematol Oncol 2011; 4: 13.
15) Yokota S, Kiyoi H, Nakao M, Iwai T, Misawa T, Okuda T, Sonoda Y, Abe T, Kahsima K, Matsuo Y, Naoe T. Internal tandem duplication of the FLT3 gene is preferentially seen in acute myeloid leukemia and myelodysplastic syndrome among various hematological malignancies. A study on a large series of patients and cell lines. Leukemia 1997; 11: 1605-1609.
16) Gary Gilliland D, Griffin JD. The roles of FLT3 in hematopoiesis and leukemia. Blood 2002; 100: 1532-1542.
17) Calò V, Migliavacca M, Bazan V, Macaluso M, Buscemi M, Gebbia N, Russo A. STAT proteins: from normal control of cellular events to tumorigenesis. J Cell Physiol 2003; 197: 157-168.
18) Takahashi S, Harigae H, Kaku M, Sasaki T, Licht JD. Flt3 mutation activates p21WAF1/CIP1 gene expression through the action of STAT5. Biochemical and biophysical research communications 2004; 316: 85-92.
19) Hayakawa F, Towatari M, Kiyoi H, Tanimoto M, Kitamura T, Saito H, Naoe T. Tandem-duplicated Flt3 constitutively activates STAT5 and MAP kinase and introduces autonomous cell growth in IL-3-dependent cell lines. Oncogene 2000; 19: 624-631.
20) Takahashi S, McConnell MJ, Harigae H, Kaku M, Sasaki T, Melnick AM, Licht JD. The Flt3 internal tandem duplication mutant inhibits the function of transcriptional repressors by blocking interactions with SMRT. Blood 2004; 103: 4650-4658.
21) Mizuki M, Schwäble J, Steur C, Choudhary C, Agrawal S, Sargin B, Steffen B, Matsumura I, Kanakura Y, Böhmer FD, Müller-Tidow C, Berdel WE, Serve H. Suppression of myeloid transcription factors and induction of STAT response genes by AML-specific Flt3 mutations. Blood 2003; 101: 3164-3173.
22) Bender O, Atalay A. Evaluation of anti-proliferative and cytotoxic effects of chlorogenic acid on breast cancer cell lines by real-time, label-free and high-throughput screening. Marmara Pharm J 2018; 22: 173-179.

23) Mahomoodally MF, Atalay A, Picot MCN, Bender O, Celebi E, Mollica A, Zengin G. Chemical, biological and molecular modelling analyses to probe into the pharmacological potential of Antidesma madagascariense Lam.: A multifunctional agent for developing novel therapeutic formulations. J Pharm Biomed Anal 2018; 161: 425-435.

24) Bender O, Llorent-Martínez EJ, Zengin G, Mollica A, Ceylan R, Molina-García L, Fernández-de Córdova ML, Atalay A. Integration of in vitro and in silico perspectives to explain chemical characterization, biological potential and anticancer effects of Hypericum salsugineum: A pharmacologically active source for functional drug formulations. PLoS One 2018; 13: e0197815.

25) Hatipoglu OF, Yaykasli KO, Dogan M, Yaykasli E, Bender O, Yasar T, Tapan S, Gunduz M. NF-κB and MAPKs are involved in resistin-caused ADAMTS-5 induction in human chondrocytes. Clin Invest Med 2015; 38: 248-254.

26) Bender O, Shoman ME, Ali TFS, Dogan R, Celik I, Mollica A, Hamed MI, Aly OM, Alamri A, Alanazi J, Ahemad N, SH, Malik JA, Anwar S, Atalay A, Beshr EAM. Discovery of oxindole-based FLT3 inhibitors as a promising therapeutic lead for acute myeloid leukemia carrying the oncogenic ITD mutation. Arch Pharm 2022; e2200407.

27) Kawase T, Nakazawa T, Eguchi T, Tsuzuki H, Ueno Y, Amano Y, Suzuki T, Mori M, Yoshida T. Effect of Fms-like tyrosine kinase 3 (FLT3) ligand (FL) on antitumor activity of gilteritinib, a FLT3 inhibitor, in mice xenografted with FL-overexpressing cells. Oncotarget 2019; 10: 6111-6123.

28) Zengin G, Rodrigues MJ, Abdallah HH, Custodio L, Stefanucci A, Aumeeruddy MZ, Mollica A, Rengasamy KRR, Mahomoodally MF. Combination of phenolic profiles, pharmacological properties and in silico studies to provide new insights on Silene salsuginea from Turkey. Comput Biol Chem 2018; 77: 178-186.

29) Bibi Sadeer N, Llorent-Martínez EJ, Bene K, Fawzi Mahomoodally M, Mollica A, Ibrahime Sinan K, Stefanucci A, Ruiz-Riaguas A, Fernández-de Córdova ML, Zengin G. Chemical profiling, antioxidant, enzyme inhibitory and molecular modelling studies on the leaves and stem bark extracts of three African medicinal plants. J Pharm Biomed Anal 2019; 174: 19-33.

30) Friesner RA, Murphy RB, Repasky MP, Frye LL, Greenwood JR, Halgren TA, Sanschagrin PC, Mainz DT. Extra precision glide: Docking and scoring incorporating a model of hydrophobic enclosure for protein– ligand complexes. J Med Chem 2006; 49: 6177-6196.

31) Greenwood JR, Calkins D, Sullivan AP, Shelley JC. Towards the comprehensive, rapid, and accurate prediction of the favorable tautomeric states of drug-like molecules in aqueous solution. J Comput Aided Mol Des 2010; 24: 591-604.

32) Sterling T, Irwin JJ. ZINC 15 - Ligand Discovery for Everyone. J Chem Inf Model 2015; 55: 2324-2337.

33) Stefanucci A, Luisi G, Zengin G, Macedonio G, Dimmito MP, Novellino E, Mollica A. Discovery of arginine-containing tripeptides as a new class of pancreatic lipase inhibitors. Future Med Chem 2019; 11: 5-19.

34) Mollica A, Zengin G, Durdagi S, Ekhteiari Salmas R, Macedonio G, Stefanucci A, Dimmito MP, Novellino E. Combinatorial peptide library screening for discovery of diverse α-glucosidase inhibitors using molecular dynamics simulations and binary QSAR models. J Biomol Struct Dyn 2019; 37: 726-740.

35) Zengin G, Mahomoodally MF, Sinan KI, Sadeer N, Maggi F, Caprioli G, Angeloni S, Mollica A, Stefanucci A, Ak G, Cakılcıoglu U, Polat R, Akan H. Evaluation of chemical constituents and biological properties of two endemic Verbascum species. Process Biochem 2021; 108: 110-120.

36) Loeffler JR, Fernández-Quintero ML, Schauperl M, Liedl KR. STACKED–S olvation T heory of A romatic C omplexes as K ey for E stimating D rug Binding. J Chem Inf Model 2020; 60: 2304-2313.

37) Pettersen EF, Goddard TD, Huang CC, Couch GS, Greenblatt DM, Meng EC, Ferrin TE. UCSF Chimera – a visualization system for exploratory research and analysis. J Comput Chem 2004; 25: 1605-1612.

38) Evans DJ, Holian BL. The nose-hoover thermostat. J Chem Phys 1985; 83: 4069-4074.

39) Parrinello M, Rahman A. Polymorphic transitions in single crystals: A new molecular dynamics method. J Appl Phys 1981; 52: 7182-7190.

40) Liu X, Shi D, Zhou S, Liu H, Liu H, Yao X. Molecular dynamics simulations and novel drug discovery. Expert Opin Drug Discov 2018; 13: 23-37.

41) Celik I, Erol M, Duzgun Z. In silico evaluation of potential inhibitory activity of remdesivir, favipiravir, ribavirin and galidesivir active forms on SARS-CoV-2 RNA polymerase. Mol Divers 2022; 26: 279-292.

42) Daina A, Michielin O, Zoete V. SwissADME: a free web tool to evaluate pharmacokinetics, drug-likeness and medicinal chemistry friendliness of small molecules. Sci Rep 2017; 7: 1-13.

43) Daina A, Michielin O, Zoete V. iLOGP: a simple, robust, and efficient description of n-octanol/water partition coefficient for drug design using the GB/SA approach. J Chem Inf Model 2014; 54: 3284-3301.

44) Daina A, Zoete V. A boiled-egg to predict gastrointestinal absorption and brain penetration of small molecules. ChemMedChem 2016; 11: 1117-1121.

45) Lipinski CA. Lead-and drug-like compounds: the rule-of-five revolution. Drug Discov Today Technol 2004; 1: 337-341.

46) Doganc F, Celik I, Eren G, Kaiser M, Brun R, Goker H. Synthesis, in vitro antiprotozoal activity, molecular docking and molecular dynamics studies of some new monocationic guanidinobenzimidazoles. Eur J Med Chem 2021; 221: 113545.

47) Nepstad I, Hatfield KJ, Grønningsæter IS, Reikvam H. The PI3K-Akt-mTOR signaling pathway in human acute myeloid leukemia (AML) cells. Int J Mol Sci 2020; 21: 2907.

48) Cai H, Ren L, Wang Y, Zhang Y. Beta-Elemene Reduces the Malignancy of Non-Small Cell Lung Cancer by Enhancing C3orf21 Expression. Front Oncol 2021; 11: 571476.

49) Zhu Y, Hu J, Shen F, Shen H, Liu W, Zhang J. The cytotoxic effect of β-elemene against malignant glioma is enhanced by base-excision repair inhibitor methoxyamine. J Neurooncol 2013; 113: 375-384.

50) Chen W, Lu Y, Wu J, Gao M, Wang A, Xu B. Beta-elemene inhibits melanoma growth and metastasis via suppressing vascular endothelial growth factor-mediated angiogenesis. Cancer Chemother Pharmacol 2011; 67: 799-808.

51) Li X, Wang G, Zhao J, Ding H, Cunningham C, Chen F, Flynn DC, Reed E, Li QQ. Antiproliferative effect of beta-elemene in chemoresistant ovarian carcinoma cells is mediated through arrest of the cell cycle at the G2-M phase. Cell Mol Life Sci 2005; 62: 894-904.

52) Li QQ, Wang G, Zhang M, Cuff CF, Huang L, Reed E. Beta-Elemene, a novel plant-derived antineoplastic agent, increases cisplatin chemosensitivity of lung tumor cells by triggering apoptosis. Oncol Rep 2009; 22: 161-170.

53) Wu Z, Wang T, Zhang Y, Zheng Z, Yu S, Jing S, Chen S, Jiang H, Ma S. Anticancer effects of β-elemene with hyperthermia in lung cancer cells. Exp Ther Med 2017; 13: 3153-3157.

54) Ozaki T, Nakagawara A. Role of p53 in Cell Death and Human Cancers. Cancers 2011; 3: 994-994.

55) Pan Z, Xie Y, Bai J, Lin Q, Cui X, Zhang N. Bufalin suppresses colorectal cancer cell growth through promoting autophagy in vivo and in vitro. RSC Adv 2018; 8: 38910-38918.

56) Yun CW, Lee SH. The Roles of Autophagy in Cancer. Int J Mol Sci 2018; 19: 3466.

57) Nazio F, Bordi M, Cianfanelli V, Locatelli F, Cecconi F. Autophagy and cancer stem cells: molecular mechanisms and therapeutic applications. Cell Death Differ 2019; 26: 690-702.

58) Bender O, Atalay A. Chapter 28 - Polyphenol chlorogenic acid, antioxidant profile, and breast cancer. Cancer (Second Edition), Academic Press, 2021; 311-321.

59) Chien J, Campioni M, Shridhar V, Baldi A, Chien J. HtrA Serine Proteases as Potential Therapeutic Targets in Cancer. Curr Cancer Drug Targets 2009; 9: 451-451.

60) Zhai B, Zeng Y, Zeng Z, Zhang N, Li C, Zeng Y, You Y, Wang S, Chen X, Sui X. Drug delivery systems for elemene, its main active ingredient β-elemene, and its derivatives in cancer therapy. Int J Nanomedicine 2018; 13: 6279.

61) Sankar M, Ramachandran B, Pandi B, Mutharasappan N, Ramasamy V, Prabu PG, Shanmugaraj G, Wang Y, Muniyandai B, Rathinasamy S, Chandrasekaran B, Bayan MF, Jeyaraman J, Halliah GP, Ebenezer SK. In silico screening of natural phytocompounds towards identification of potential lead compounds to treat COVID-19. Front Mol Biosci 2021; 8: 637122.